Targeting a metalloprotease-PAR1 signaling system with cell-penetrating pepducins inhibits angiogenesis, ascites, and progression of ovarian cancer

Anika Agarwal,[1,2] Lidija Covic,[1,2] Leila M. Sevigny,[1,4] Nicole C. Kaneider,[1] Katherine Lazarides,[1] Gissou Azabdaftari,[3] Sheida Sharifi,[3,5] and Athan Kuliopulos[1,2,4]

[1]Molecular Oncology Research Institute, [2]Division of Hematology-Oncology, Department of Medicine, Tufts Medical Center; [3]Department of Pathology, Tufts-New England Medical Center; [4]Departments of Biochemistry and Genetics, Tufts University Medical School, Boston, Massachusetts and [5]Department of Pathology Mount Auburn Hospital Cambridge, Massachusetts

Abstract

Gene chip and proteomic analyses of tumors and stromal tissue has led to the identification of dozens of candidate tumor and host components potentially involved in tumor-stromal interactions, angiogenesis, and progression of invasive disease. In particular, matrix metalloproteases (MMP) have emerged as important biomarkers and prognostic factors for invasive and metastatic cancers. From an initial screen of benign versus malignant patient fluids, we delineated a metalloprotease cascade comprising MMP-14, MMP-9, and MMP-1 that culminates in activation of PAR1, a G protein-coupled protease-activated receptor up-regulated in diverse cancers. In xenograft models of advanced peritoneal ovarian cancer, PAR1-dependent angiogenesis, ascites formation, and metastasis were effectively inhibited by i.p. administration of cell-penetrating pepducins based on the intracellular loops of PAR1. These data provide an *in vivo* proof-of-concept that targeting the metalloprotease-PAR1 signaling system may be a novel therapeutic approach in the treatment of ovarian cancer. [Mol Cancer Ther 2008;7(9):2746–57]

Received 2/19/08; revised 6/5/08; accepted 6/19/08.

Grant support: NIH grants CA122992, HL64701, and HL57905 (A. Kuliopulos) and CA104406 (L. Covic) and Susan G. Komen Breast Cancer Foundation (A. Kuliopulos).

The costs of publication of this article were defrayed in part by the payment of page charges. This article must therefore be hereby marked *advertisement* in accordance with 18 U.S.C. Section 1734 solely to indicate this fact.

Requests for reprints: Athan Kuliopulos, Molecular Oncology Research Institute, Tufts Medical Center, Box 7510, Boston, MA 02111. E-mail: athan.kuliopulos@tufts.edu

doi:10.1158/1535-7163.MCT-08-0177

Introduction

Ovarian cancer is a particularly deadly malignancy, because the vast majority of patients are diagnosed well after the cancer has spread throughout the peritoneal cavity (1). Despite excellent initial response rates to chemotherapy, most patients experience relapses due to drug resistance. This has sparked an upsurge in interest in developing targeted therapies that block key signaling pathways involved in tumor-stromal interactions, tumor vascularity, and invasion (2, 3). Abundant evidence has pointed to matrix metalloproteases (MMP) as playing critical roles in invasion, blood vessel penetration, and metastasis of many solid tumors including ovarian cancer (4, 5). MMPs are zinc-dependent proteases secreted by both tumor and host cells that are required for tumor cell invasion through the basement membrane and stromal tissue. Secreted MMPs are produced in the proform as inactive zymogens, which are activated on the cell surface by other proteases and membrane-tethered MMPs (4). However, the mechanism of activation of individual pro-MMPs remains largely unknown and may differ depending on the tumor type and stage. Human ovarian cancer cells and surrounding stroma have been shown to secrete proMMP-2 and proMMP-9 (6, 7) and the increased expression of these gelatinases is associated with high invasive and metastatic potential (8, 9) and short overall survival of ovarian cancer patients (10). Peritoneal inflammatory cells also supply metalloproteases such as macrophage-derived MMP-9, which increases tumorigenesis and angiogenesis in genetically modified mice (11).

In addition to MMP-2 and MMP-9, one of the most promising of the new candidate biomarkers for metastatic and invasive cancer is the fibroblast collagenase, MMP-1. High MMP-1 expression in tumors is associated with poor prognosis in patients with colorectal, esophageal, and breast cancer (12–14). MMP-1 was also identified as a predictive marker for breast cancer where it is expressed in reactive stromal tissue and ductal lavage fluids of patients with no prior history of breast cancer (15). A commonly occurring G/2G promoter polymorphism, which causes enhanced *MMP1* transcription (16), was recently shown to be associated with shortened disease-free and overall 5-year survival in ovarian cancer patients (17); however, it is not clear whether MMP-1 collagenase plays a direct role in the progression of ovarian cancer.

From a screen of fluids derived from patients with benign versus malignant ovarian diseases, a metalloprotease cascade was identified which culminates in activation of proMMP-1 to MMP-1. MMP-1 in turn directly activated PAR1 (18), a cell surface receptor coupled to G proteins (19). PAR1 is not normally expressed in nonmalignant

epithelia including ovarian (20, 21) but was found to be highly up-regulated in invasive ovarian carcinomas *in vitro* and when passaged in mice. PAR1-dependent angiogenesis and ascites formation, invasion, and metastasis were effectively inhibited downstream of the MMP cascade by a cell-penetrating lipopeptide ''pepducin'' based on the third intracellular loop of PAR1. These results provide *in vivo* evidence that PAR1 may be potential therapeutic target in ovarian cancer.

Materials and Methods

Pepducins

N-palmitoylated peptides, P1pal-7 ($C_{15}H_{31}$CONH-KKSRALF-NH_2), P1pal-12 ($C_{15}H_{31}$CONH-RCLSSSA-VANRS-NH_2), and P1pal-19EE ($C_{15}H_{31}$CONH-RCESS-SAEANRS KKERELF-NH_2), were synthesized by standard Fmoc synthetic methods with COOH-terminal amides. Palmitic acid was dissolved in 50% *N*-methylpyrolidone/50% methylene chloride and coupled overnight to the deprotected NH_2-terminal amine of the peptide. After cleavage from the resin, palmitoylated peptides were purified to >95% purity by C_{18} or C_4 reverse-phase high-performance liquid chromatography as before (22).

RNA Interference

RNA interference (RNAi) reagents have been described previously and characterized: *MMP-9* (5′-CAUCAC-CUAUUGGAUCCAAdTdT-3′; ref. 23), *MMP-14* (5′-AUG-CAGAAGUUUUACGGCUUGUU-3′; ref. 24), firefly *luciferase* (5′-CGTACGCGGAATACTTCGA-3′), and *PAR1* (5′-AAGGCUACUAUGCCUACUACU-3′; ref. 18). The *PAR3* RNAi SMART pool L-005491 was synthesized by Dharmacon. Total RNA was extracted for reverse transcription-PCR from OVCAR-4 cells with RNeasy mini kit (Qiagen). cDNA was prepared with 5 μg total RNA using MMLV reverse transcriptase. The desired products were amplified using Taq polymerase and the following primers: *hMMP-1* sense 5′-CGACTCTAGAAACACAAGAG-CAAGA-3′ and antisense 5′-AAGGTTAGCTTACTGTCA-CACGCTT-3′, *hMMP-2* sense 5′-GTGCTGAAGGACACA-CTAAAGAAGA-3′ and antisense 5′-TTGCCATCCTTCT-CAAAGTTGTAGG-3′, *hMMP-9* sense 5′-CACTGTCCACC-CCTCAGAGC-3′ and antisense 5′-GCCACTTGTCGGCGA-TAAGG-3′, *hMMP14* sense 5′-GCTTGCAAGTAACAGG-CAAA-3′ and antisense 5′-AAATTCTCCGTGTCCATC-CA-3′ (as described in refs. 18, 24), *hMMP-8* sense 5′-GA-CGCTTCCATTTCTGCTCTTACTCCAT-3′ and antisense 5′-TCCCCGTCACATTCAACCCAAAAA-3′, and *MMP-3* sense 5′-GATCTCTTCATTTTGGCCATCTCTTC-3′ and antisense 5′-CTTCCAGTATTTGTCCTCTACAAAGAA-3′.

Cell Culture

OVCAR-4, SKOV-3, OVCAR-3, IGROV-1, OVCAR-5, and OVCAR-8 cells were obtained from the National Cancer Institute. NIH-3T3 murine fibroblasts were from the American Type Culture Collection. Cells were grown in RPMI with 10% fetal bovine serum and transfected with OligofectAMINE using 20 μmol/L RNAi per 100 mm plate. Migration assays were conducted 48 h following transfection. Human recombinant interleukin-8 was expressed in *Escherichia coli* using the pET31 system (25) and purified and reconstituted as described previously (26).

Flow Cytometry

Rabbit polyclonal PAR1 and PAR3 antibodies were purified by peptide affinity chromatography as described previously (27). FITC-conjugated goat anti-rabbit antibody was purchased from Zymed. Flow cytometry was done on ovarian carcinoma cells as before (27, 28).

Cell Migration and MMP Assays

Ovarian and hepatic ascites, ovarian cystic fluid, and pleural effusions were collected from 16 patients with all patient identifiers removed as approved by the Tufts Medical Center Institutional Review Board (Supplementary Table S1).[6] Conditioned medium was prepared from fibroblasts or OVCAR-4 cells after 2 days of cell culture as described (18). Chemotactic migration and chemoinvasion (29) assays were conducted using a 8 μm pore size Transwell apparatus (Corning) as described previously (27). Chemotactic index measurements (ratio between the distance of migration toward chemoattractants over that toward medium alone) were done with a 48 blindwell microchemotaxis chamber (Neuroprobe) equipped with 8 μm pore nitrocellulose filters as described previously (26). Pure proMMP-1, proMMP-2, proMMP-3, proMMP-7, and proMMP-9 were obtained from EMD BioSciences. MMP-200 was from Enzyme Systems Products, and FN-439 (MMP Inh-1), MMP 2 Inh, MMP 9/13 Inh-1, MMP-3 Inh-III were from Calbiochem. Human α-thrombin was from Haematologic Technologies. Stock solutions of 400 nmol/L proMMP-1 were activated with 2 mmol/L APMA in 50 mmol/L Tris (pH 7.7), 5 mmol/L $CaCl_2$, 0.2 mol/L NaCl, and 50 μmol/L $ZnCl_2$ at 37°C for 30 min and then transferred to an ice bath before use. Before migration assays, the APMA was removed by overnight dialysis in 10 kDa MWCO Mini Slide-A-Lyzers (Pierce) at 4°C. Quantikine human proMMP-1, total MMP-2, total MMP-3, total MMP-8, total MMP-9, and total MMP-13 ELISAs were purchased from R&D Systems and was used according to the manufacturer's protocol. Collagenase activity was assayed from lysed cells and in conditioned medium by measuring the cleavage of fluorescein conjugated DQ collagen (Molecular Probes). Collagenase assays contained 10 μg DQ collagen in 50 mmol/L Tris-HCl (pH 7.6), 150 mmol/L NaCl, 5 mmol/L $CaCl_2$, and 0.2 mmol/L NaN_3 and cleavage was monitored at 538 nm using a fluorescence microplate reader with excitation at 485 nm at 25°C. One unit of collagenase activity was defined as the cleavage of 1 μg collagen/min at 25°C.

Endothelial Monolayer Permeability Assays

Immortalized human umbilical vein endothelial cells (EA.hy926) were plated on 3 μm polycarbonate Transwell membranes (Corning) in EBM2 supplemented with 10% fetal bovine serum. After reaching confluence, the cell

[6] Supplementary material for this article is available at Molecular Cancer Therapeutics Online (http://mct.aacrjournals.org/).

coated membranes were placed into a dual chamber system and were either treated with MMP-1 or conditioned medium from peritoneal fibroblasts (HPF) in the presence or absence of 5 μmol/L FN-439, 5 μmol/L RWJ-56110, or 3 μmol/L P1pal-7. After a 2 h incubation period, the medium in the upper chamber was removed and DMEM containing 30 mg/mL Evans blue was added to the upper well and PBS was added to the lower compartment of the chamber. After 15 min incubation, Evans blue was quantified in the lower wells by A_{650}.

Peritoneal Ovarian Tumor Models

All animal experiments were conducted in full compliance with Tufts Medical Center Institutional Animal Care and Use Committee. Female NCR *nu/nu* mice (5-7 weeks) were purchased from Taconic Farms. Mice were injected into the peritoneal cavity with 1.5 million OVCAR-4 or SKOV-3 cells. Animals were subsequently treated every other day with either i.p. injections of P1pal-7 pepducin or FN-439 in 100 μL of 10% DMSO vehicle with or without concomitant docetaxel. At the end of 6 weeks, tumors and organs were excised from euthanized mice, fixed in 10% formalin/PBS, and embedded in paraffin. Tissue sections (5 μm) from omentum, diaphragm, abdominal, and thoracic organs were prepared and stained with H&E or immunostained using a rabbit polyclonal anti-von Willebrand factor (DakoCytomation) for microvessel quantification and staged in a blinded manner by two independent pathologists.

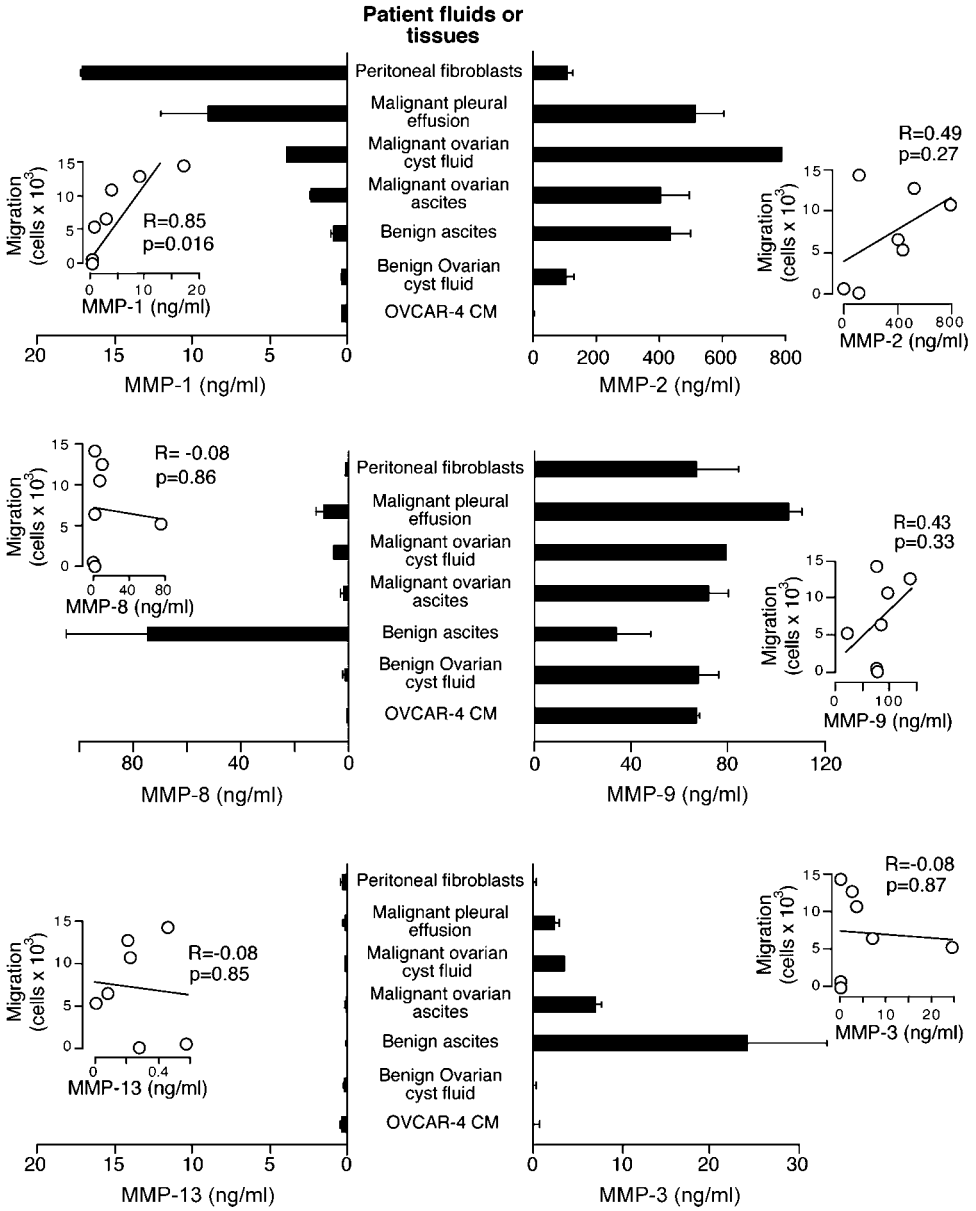

Figure 1. ProMMP-1 in patient fluids correlates with ovarian carcinoma cell migration. Various fluids were collected from 16 patients with benign or malignant disease. ProMMP-1, total MMP-2 (proform and active form), total MMP-3 (proform and active form), total MMP-8 (proform and active form), total MMP-9 (proform and active form), and proMMP-13 levels were measured by ELISA from malignant ascites (n = 4), malignant pleural effusion (n = 4), benign ascites (n = 4), benign ovarian cyst (n = 3), peritoneal fibroblasts (n = 2), and malignant ovarian cyst (n = 1). Primary peritoneal fibroblasts were cultured from ascitic taps obtained from patients with ovarian cancer. Conditioned medium from 80% confluent peritoneal fibroblasts or OVCAR-4 ovarian carcinoma cells was collected after 2 d in RPMI. Mean ± SE. *Inserts,* linear correlation of MMP levels (*X axis*) versus migration of OVCAR-4 cells (*Y axis*) toward the various fluids is shown for each MMP. OVCAR-4 cells (50,000) were allowed to migrate for 18 h toward each of the patient fluids or the conditioned medium from peritoneal fibroblasts or OVCAR-4 cells using 8 μm pore Transwell apparatus. Statistical analyses were conducted by linear regression using the SAS System and the CORR procedure.

Results and Discussion

MMPs in Benign versus Malignant Ovarian Fluids

Patients with ovarian cancer often produce copious amounts of peritoneal ascites or cystic fluid, which may contain metalloproteases that aid in the dissemination of the cancer. Fluid was collected from the peritoneal cavity (ascites), ovarian cysts, or pleura from 16 patients with malignant or benign diseases. Protein levels of the collagenases (proMMP-1, total MMP-8, and proMMP-13), gelatinases (total MMP-2 and total MMP-9), and stromelysin (total MMP-3) were then measured in the patient fluids. Of the six MMPs tested, proMMP-1 levels had the strongest positive correlation with malignancy (Fig. 1). Likewise, there was a significant correlation between proMMP-1 levels in the patient samples and ability to induce migration of highly invasive OVCAR-4 carcinoma cells ($R = 0.85$; $P = 0.016$). Malignant ovarian cyst fluid and ovarian ascites had proMMP-1 levels that were 8- to 13-fold higher than those in benign ovarian cyst fluid. Conditioned medium from peritoneal fibroblasts isolated from ovarian cancer patients had up to 200-fold higher proMMP-1 levels than medium from the OVCAR-4 cancer cells themselves (Fig. 1). Conversely, protein levels of the other collagenases, MMP-8 and MMP-13, did not correlate with either malignancy or ability to induce migration. Levels of the MMP-2 gelatinase were 90- to 550-fold higher than proMMP-1 in the patient fluids but did not correlate as strongly with malignancy or migration. MMP-9 gelatinase was abundant in nearly all tested benign and malignant patient fluids (71 ± 20 ng/mL) and was produced at very high levels by OVCAR-4 cells. MMP-3 levels did not correlate with malignancy or migration.

PAR1, a Receptor for MMP-1, Is Correlated with Invasive Propensity of Ovarian Cancers

A recent study found that the G protein-coupled receptor, PAR1, is cleaved by MMP-1, which promotes breast cancer migration and invasion (18). To investigate whether PAR1 might play a role in metalloprotease-dependent chemotaxis of ovarian carcinoma cells, we characterized six ovarian cancer cell lines from the NCI-60 panel for PAR1 surface expression and correlated expression with cell migration toward fibroblast conditioned medium. There was a strong positive correlation ($R = 0.96$; $P = 0.0006$) between PAR1 expression and migration of OVCAR-5, OVCAR-3, SKOV-3, IGROV-1, OVCAR-8, and OVCAR-4 ovarian cancer cell lines (Fig. 2A). In contrast, there was a poor correlation ($R = 0.33$; $P = 0.47$) between the closely homologous PAR3 receptor (Fig. 2A) and migration of ovarian cancer cells to the fibroblast conditioned medium. OVCAR-4 cells had the highest levels of PAR1 surface expression and gave a robust calcium signal to the PAR1 ligand TFLLRN (data not shown). We also tested whether there was a correlation between the levels of a particular MMP in the patient fluids and chemoinvasion (29) of the ovarian carcinoma cells through Matrigel. Consistent with the migration data, the only significant positive correlation between chemoinvasion and MMP level was observed for proMMP-1 and the high PAR1-expressing OVCAR-4 and IGROV-1 cells (Supplementary Table S2).

Metastatic spread of cancer cells in mice often results in altered expression of malignancy-associated genes; therefore, we tested whether passage of OVCAR-4 cells in the peritoneal cavity of nude mice would increase expression of PAR1. OVCAR-4ip1 cells, harvested at 40 days from nude mice, had a 2.3-fold further increase in migration and a corresponding 2.5-fold further increase in surface expression of PAR1 (Fig. 2A). In contrast, surface expression of PAR3 dropped by 50% in the i.p. passaged OVCAR-4 cells relative to the parent OVCAR-4 cells. Gene silencing of *PAR1* in the OVCAR-4ip1 and parental OVCAR-4 cells with RNAi caused a 45% to 77% decrease in median surface expression of PAR1 relative to luciferase control RNAi-treated cells (Supplementary Fig. S1A) with an attendant 60% to 75% loss in cell migration (Fig. 2B). PAR3 RNAi treatment (Supplementary Fig. S1B) had no effect on the migration of either OVCAR4 or OVCAR-4ip1 cells (Fig. 2). To validate the MMP1-PAR1 signaling axis, OVCAR-4 cells were treated with either PAR1 or luciferase RNAi for 48 h and then tested for ability to migrate toward MMP-1. The 2.3-fold increased migration toward 0.3 nmol/L MMP-1 was completely blocked with *PAR1* RNAi treatment of the OVCAR-4 cells (Fig. 2C). To provide evidence that the decreased migration was a PAR1-specific event, we found that chemotactic migration of the OVCAR-4 cells toward IL-8 was unaffected by *PAR1* RNAi treatment relative to *luciferase* RNAi (Supplementary Fig. S1C).

PAR1 Pepducins Inhibit Migration of Ovarian Cancer Cells toward Malignant Ascites Fluid

To block PAR1-dependent migration of ovarian carcinoma cells toward ascites fluid from patients with ovarian cancer or fibroblast medium, we used cell-penetrating pepducin antagonists based on the intracellular loops of PAR1 (22, 30). Pepducins are cell-penetrating lipopeptide conjugates based on the sequences of the intracellular loops of PAR1 and other G protein-coupled receptors (22, 26, 30, 31). After delivering its cargo across the plasma membrane, the lipid moiety anchors the compound to the lipid bilayer, thereby concentrating the pepducin to the target receptor-G protein interface (32). The P1pal-12 pepducin is a *N*-palmitoylated peptide based on the amino-terminal portion of the third intracellular loop of PAR1 that interdicts signaling between PAR1 and internally located G proteins (22). In addition, we tested a carboxyl-terminal third intracellular loop pepducin, P1pal-7, which is a full antagonist of PAR1, and a negative control PAR1 pepducin, P1pal-19E (22). Plpal-12 and P1pal-7 blocked 90% to 94% of OVCAR-4 migration toward human ovarian ascites and fibroblast conditioned medium, whereas P1pal-19E was without effect (Fig. 2D). Likewise, a small-molecule ligand-based antagonist of PAR1, RWJ-56110 (33), strongly inhibited migration of the OVCAR-4 cells. We also tested the ability of the PAR1-based pepducins to inhibit migration of other ovarian carcinoma cell lines to either malignant human ascites fluid or fibroblast medium.

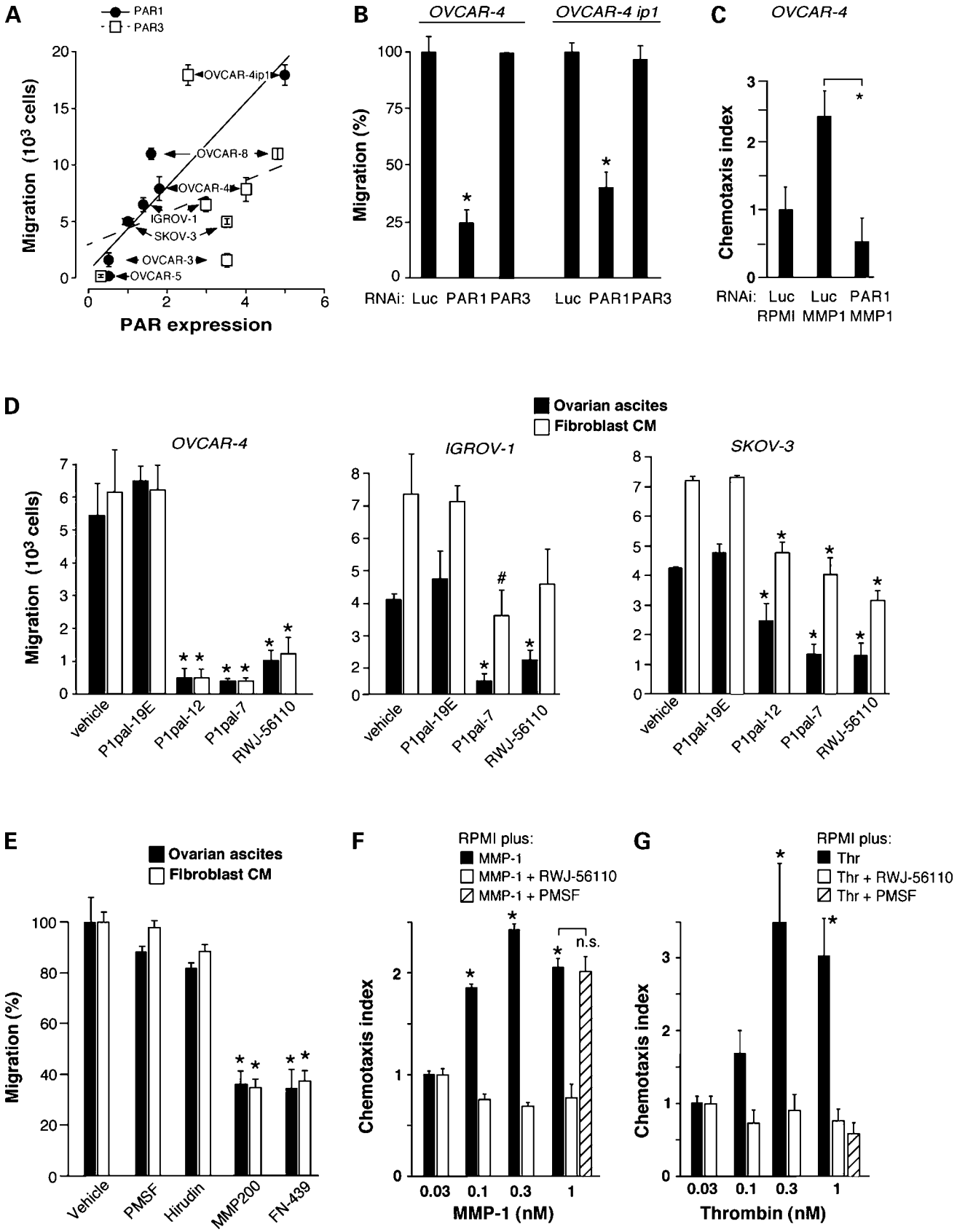

IGROV-1 cells were inhibited by up to 80% with the PAR1 pepducins or RWJ-56110, whereas SKOV-3 was inhibited by 33% to 70% (Fig. 2D). The less pronounced inhibition of migration of the SKOV-3 cells by the PAR1 antagonists was correlated with the lower PAR1 expression levels in those cells compared with the high PAR1-expressing OVCAR-4 cells. Addition of the PAR1 antagonists had no effect on the migration of the very low PAR1-expressing OVCAR-3 cells (Supplementary Fig. S2).

MMP-1 Activity from Malignant Ascites Fluid Stimulates the Migration of Ovarian Carcinoma Cells

PAR1 has been shown to be activated by several serine proteases from blood such as thrombin, plasmin, and activated protein C or by fibroblast-secreted MMP-1 (18, 28, 34). To provide evidence that the MMP-1 activity derived from the human ascites was responsible for the PAR1-dependent migration of the OVCAR-4 cells, a panel of protease inhibitors that block serine proteases (polymethylsulfonyl fluoride, broad-spectrum serine protease inhibitor; hirudin, specific thrombin inhibitor) or Zn^{2+}-dependent MMPs (MMP-200, broad-spectrum MMP inhibitor; FN-439, inhibitor of MMP-1) were assessed for their ability to block migration. As shown in Fig. 2E, neither hirudin nor polymethylsulfonyl fluoride inhibited migration, whereas MMP-200 and FN-439 prevented 65% of migration of OVCAR-4 cells toward ascites fluid from patients with ovarian cancer or conditioned medium from fibroblasts. The 35% to 40% residual motility of the OVCAR-4 cells may be due to other chemotactic factors or proteases that are not blocked by the protease inhibitors employed. To confirm that proteolytic activation of PAR1 is capable of stimulating migration of OVCAR-4 cells, we added exogenous activated MMP-1 or thrombin to serum-free medium in the lower chamber of the chemotaxis apparatus. We found that low concentrations of MMP-1 or thrombin induced cell motility of OVCAR-4 with a peak at 0.3 nmol/L for both proteases (Fig. 2F-G). MMP-1 and thrombin induction of OVCAR-4 cell mobility was abolished with the PAR1 inhibitor, RWJ-56110. MMP1-induced migration was unaffected by polymethylsulfonyl fluoride, whereas thrombin-induced migration was completely blocked (Fig. 2F-*G*). Together, these data indicate that the observed PAR1-dependent chemotaxis of the ovarian carcinoma cells toward MMP-1 is independent of serine proteases.

Upstream Roles of MMP-9 and MMP-14 in Activating MMP1-Dependent Migration of Ovarian Carcinoma Cells

A panel of proMMPs were individually screened for ability to stimulate chemotactic migration of OVCAR-4 ovarian carcinoma cells. We found that proMMP-1 zymogen added to serum-free medium in the bottom well was also able to induce nearly a 100% increase in chemotactic migration of OVCAR-4 cells (Fig. 3A). Unlike proMMP-1, addition of proMMP-2, proMMP-3, proMMP-7, or proMMP-9 zymogens to RPMI in the bottom well was not able to confer chemotaxis to the OVCAR-4 cells. A panel of metalloprotease inhibitors was used to determine whether active MMPs produced by the OVCAR4 cells themselves were essential for the chemotaxis toward proMMP-1. FN-439 completely blocked the ability of proMMP-1 to induce migration of the OVCAR-4 cells (Fig. 3B), indicating that active MMP-1 was required. Inhibitors against MMP-2 and MMP-3 were without effect; however, the MMP9/13 inhibitor completely blocked proMMP1-induced migration. Reverse transcription-PCR showed that the OVCAR-4 cells did not express *MMP-1, MMP-2, MMP-3*, or *MMP-8* but did express mRNA for *MMP-9* (Fig. 3C), consistent with the ELISA results in Fig. 1. Together, these data suggested that the MMP-9 produced by the OVCAR-4 cells might be required for activating exogenous proMMP-1 to MMP-1.

To provide direct evidence that MMP-9 from OVCAR-4 cells was required for MMP1-dependent migration, we suppressed *MMP-9* expression using a previously described RNAi (Supplementary Fig. S1D; ref. 23). As shown in Fig. 3D, proMMP1-dependent migration, but not MMP1-migration, was nearly completely suppressed by *MMP-9* RNAi treatment of the OVCAR4 cells compared with *luciferase* RNAi controls. To show that MMP-9 was directly activating proMMP-1, we measured *in situ* production of collagenase activity from OVCAR-4 medium. Addition of proMMP-1 to OVCAR4 cells significantly enhanced

Figure 2. MMP1-PAR1-dependent migration of ovarian cancer cells toward malignant ascites fluid. **A,** surface PAR1 and PAR3 expression of the NCI-60 ovarian cancer cell lines ($n = 6$) was measured by flow cytometry as before (27) and correlated with migration toward fibroblast-produced conditioned medium. Ovarian cancer cells (50,000) were seeded onto 8 μm pore membrane in the upper well of a Transwell apparatus and allowed to migrate for 5 h toward conditioned medium from NIH-3T3 fibroblasts. PAR1: $R = 0.96$; $P = 0.0006$. PAR3: $R = 0.33$; $P = 0.47$. **B,** silencing of PAR1 expression in OVCAR-4 and OVCAR-4ip1 cells with *PAR1* RNAi inhibits migration toward fibroblast conditioned medium. OVCAR-4 or OVCAR-4ip1 cells were transfected with *luciferase* (*Luc*), *PAR1*, or *PAR3* RNAi for 48 h. Surface expression of PAR1 and PAR3 dropped by 45% to 77% as determined by flow cytometry, when cells were treated with their respective RNAi molecules (Supplementary Fig. S1A and B). **C,** gene silencing of *PAR1* with RNAi blocks chemotaxis of OVCAR-4 cells toward MMP-1. OVCAR-4 cells were transfected with *luciferase* or *PAR1* RNAi for 48 h and then allowed to migrate toward 0.3 nmol/L MMP-1 (APMA-activated) in RPMI/0.1% bovine serum albumin (BSA) for 18 h in a 48-well microchemotaxis chamber. Chemotaxis index is the ratio of directed over random migration through 8 μm pore filter. **D,** effect of PAR1-based pepducins on migration of OVCAR-4, IGROV-1, and SKOV-3 ovarian carcinoma cells toward malignant ascites from ovarian cancer patients or fibroblast conditioned medium. Migration toward ascites or fibroblast conditioned medium was conducted in the presence of PAR1 antagonists based on either the extracellular ligand (3 μmol/L RWJ-56110) or cell-penetrating pepducins (3 μmol/L) derived from the PAR1 third intracellular loop (P1pal-12, P1pal-7, or control P1pal-19EE) in 0.2% DMSO vehicle. The source of the malignant ascites was from two different patients with ovarian adenocarcinoma. **E,** migration (18 h) of OVCAR-4 cells toward fibroblast or malignant ovarian ascites in the presence of polymethylsulfonyl fluoride (100 μmol/L), hirudin (0.015 units), MMP-200 (200 nmol/L), FN-439 (5 μmol/L), or vehicle. **F** and **G,** low concentrations of MMP-1 or thrombin activate PAR1-dependent migration of OVCAR-4 cells. OVCAR-4 cells were allowed to migrate toward activated MMP-1 or thrombin (*Thr*) in RPMI/0.1% BSA for 18 h in the presence or absence of the PAR1 antagonist, 1 μmol/L RWJ-56110, or 100 μmol/L polymethylsulfonyl fluoride. Mean ± 1 SE ($n = 2$-4) with assays done in duplicate. *, $P < 0.05$; #, $P = 0.05$-0.06, Student's *t* test.

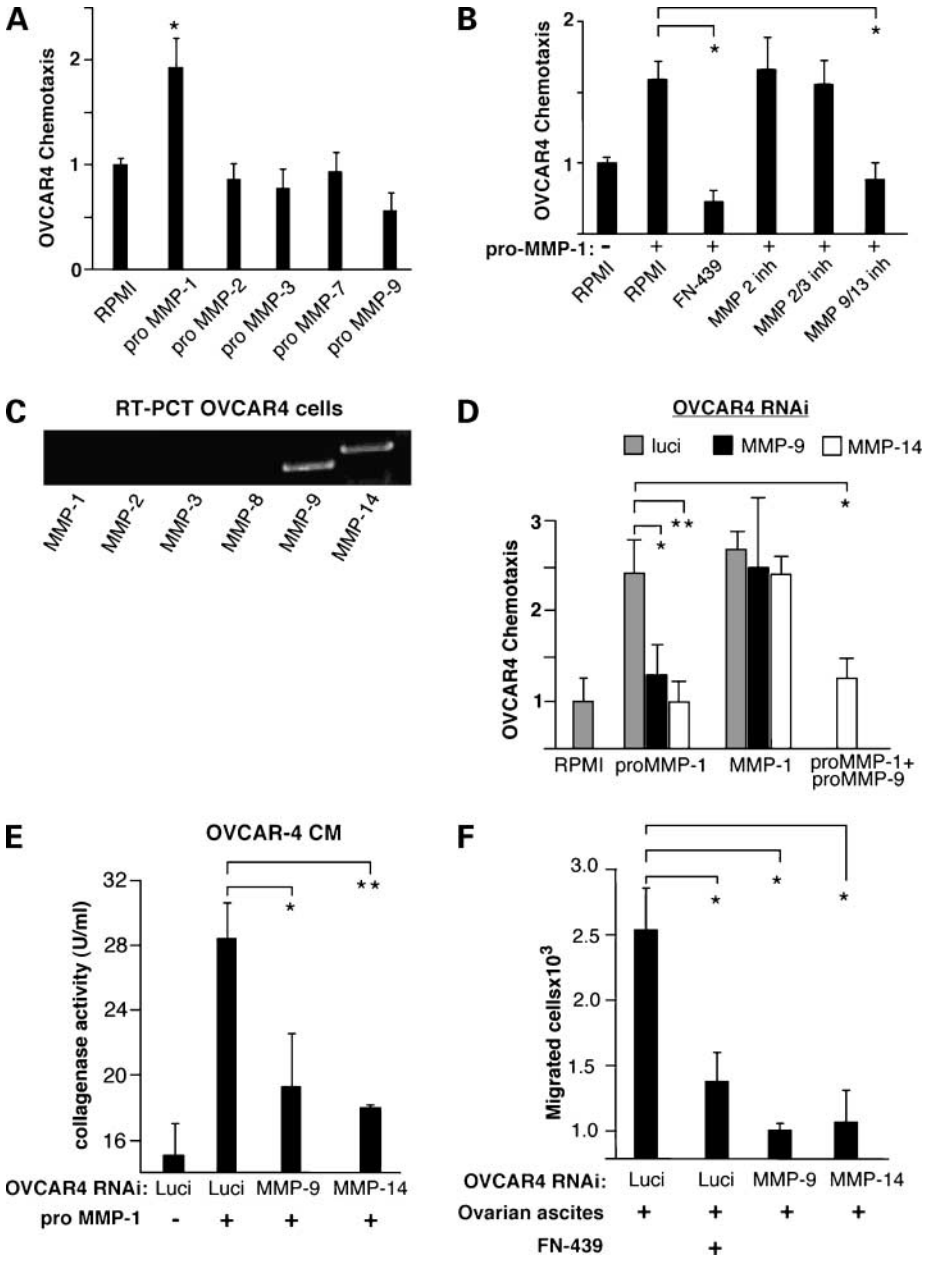

Figure 3. MMP-14 and MMP-9 activate proMMP1-dependent migration of ovarian cancer cells. **A,** OVCAR-4 cells were placed in the top well of a 48-well microchemotaxis chamber and allowed to migrate for 18 h toward 20 nmol/L of each proMMP in RPMI/0.1% BSA in the bottom well. **B,** OVCAR-4 cells were allowed to migrate toward 20 nmol/L proMMP-1 in RPMI/0.1% BSA in the presence of the indicated MMP inhibitors used at ≥3-fold IC_{50}: 5 μmol/L FN-439, 5 μmol/L MMP-2 Inh, 5 μmol/L MMP2/3 Inh, and 5 nmol/L MMP9/13 Inh. **C,** total RNA was extracted from OVCAR-4 cells. cDNA was prepared and amplified with PCR primers to MMP-1, MMP-2, MMP-3, MMP-8, MMP-9, or MMP-14 and separated on a 1.5% agarose gel. **D,** OVCAR-4 ovarian cells were treated for 48 h with RNAi directed against *MMP-9, MMP-14*, or *luciferase* (*luci*) and allowed to migrate for 18 h toward 20 nmol/L proMMP-1, 0.3 nmol/L active MMP-1, or a combination of 20 nmol/L proMMP-1 and 20 nmol/L proMMP-9 in RPMI/0.1% BSA. **E,** OVCAR-4 cells were treated with RNAi against *luciferase, MMP-9*, or *MMP-14* for 48 h, cells were washed, and 20 nmol/L proMMP-1 was added in RPMI/0.1% BSA on top of the cells. Conditioned medium from the treated cells was then collected after 6 h and assayed for collagenase activity. **F,** OVCAR-4 cells treated for 48 h with the indicated RNAi were allowed to migrate for 18 h toward malignant ovarian ascites in the absence or presence of 5 μmol/L FN-439. Mean ± 1 SE (n = 2-4). *, $P < 0.05$; **, $P < 0.01$, Student's t test.

collagenase activity by 13 ± 2 units/mL above baseline (Fig. 3E). Conversely, knockdown of *MMP-9* expression from OVCAR-4 cells with RNAi inhibited 70% of the proMMP1-dependent collagenase activity.

Tumor-derived membrane-tethered MMP-14 (35, 36) is known to convert proMMP-2 to MMP-2 (37–39) and may also be involved in the activation of the related proMMP-9 (40). We found that *MMP-14* mRNA was expressed in the OVCAR-4 cells (Fig. 3C). Therefore, we examined whether MMP-14 was also required for the promigratory effects of proMMP-1. As shown in Fig. 3D, treatment of OVCAR-4 cells with a RNAi against *MMP-14* (24) completely suppressed the promigratory effects of proMMP-1 and could be complemented by exogenous MMP-1 but not by proMMP-9 plus proMMP-1. Similarly, *MMP-14* gene suppression (Supplementary Fig. S1E) inhibited 80% of proMMP1-derived collagenase activity from OVCAR-4 cells (Fig. 3E). Taken together, these data support a proposed cascade whereby OVCAR4-produced MMP-14 and MMP-9 convert proMMP-1 to MMP-1, which in turn triggers migration.

A previous study indicated that peritoneal macrophages (11) can secrete proMMP-9, and we found that MMP-9 protein was abundant in malignant peritoneal fluids. Therefore, it is possible that the proform and/or active form of MMP-9 supplied by the peritoneal fluids would be

sufficient to activate chemotaxis of the ovarian carcinoma cells without a requirement of MMP-9 or MMP-14 from the carcinoma cells. To test this possibility, the chemotactic migration assays were conducted using ascites from patients with malignant ovarian cancer. Chemotactic migration of the OVCAR-4 cells to the malignant ascites fluid was inhibited by 75% by the MMP-1 inhibitor, FN-439 (Fig. 3F). *MMP-9* or *MMP-14* RNAi treatment of the OVCAR-4 cells ablated chemotaxis of the cells toward the malignant ascites fluid. In control experiments, neither *MMP-9* nor *MMP-14* RNAi treatments had an effect on chemotactic migration of OVCAR-4 cells toward IL-8 compared with *luciferase* RNAi controls (Supplementary Fig. S1C). Together, these data indicate that MMP-9 or other MMPs from the human ascites fluid cannot complement the loss of OVCAR4-produced MMP-9 or MMP-14.

Effects of Peritoneal Fibroblast-Derived MMP-1 on PAR1-Dependent Endothelial Barrier Function

Peritoneal carcinomatosis is associated with the production of large volumes of ascitic fluid, which has a severe negative effect on quality of life of patients with advanced ovarian cancer and may aid in peritoneal dissemination and carcinomatosis. It has been postulated that the ascitic fluid arising from the peritoneal tumors is a direct result of a leaky tumor vasculature (41, 42). Endothelial PAR1 is an important modulator of endothelial barrier function (43–45) and could potentially be involved in ascites formation. Moreover, tumor-derived MMP-1 was recently shown to activate PAR1-dependent von Willebrand factor release, calcium flux, and interleukin-8 secretion from endothelial cells (46). We tested whether MMP-1 derived from patient peritoneal fibroblasts could stimulate PAR1-dependent increases in the barrier permeability of endothelial monolayers. First, we showed that addition of exogenous MMP-1 (0.5 nmol/L) caused a 50% increase in endothelial barrier permeability, which was inhibited by either the MMP-1 antagonist, FN-439, or the PAR1 antagonists, P1pal-7 or RWJ-56110 (Fig. 4A). We then incubated peritoneal fibroblast-derived conditioned medium overnight in the presence of OVCAR-4 cells. The OVCAR4-treated peritoneal fibroblast conditioned medium elicited a 2.2-fold increase in endothelial barrier permeability, which could be nearly completely inhibited by FN-439, P1pal-7, or RWJ-56110 (Fig. 4B). Taken together, these *in vitro* data suggest that MMP-1 derived from peritoneal fibroblasts can strongly stimulate PAR1-dependent increases in endothelial barrier permeability.

To test whether PAR1 was involved in ascites formation *in vivo*, we assessed the effects of 40-day treatment with the PAR1 pepducin, P1pal-7 (10 mg/kg i.p. every other day), on nude mice with OVCAR-4 peritoneal carcinomatosis. As shown in Fig. 4C and D, vehicle-treated nude mice with OVCAR-4 peritoneal tumors developed pronounced ascitic fluid accumulation (2.5 ± 0.7 mL) at the 40-day time point. Monotherapy with the P1pal-7 pepducin significantly reduced mean ascites fluid volume by 60% ($P = 0.0017$) compared with vehicle, consistent with the predicted effects of blocking endothelial PAR1 on vascular leakage. Similar results were also seen in nude mice injected i.p. with SKOV-3 cells (11, 47). All vehicle-treated mice developed ascites; however, mice treated with P1pal-7 had a trend toward reduced ascites (65%; $P = 0.137$) at the 40-day time point (Supplementary Fig. S3).

P1pal-7 Pepducin Blocks Angiogenesis of Peritoneal Ovarian Cancers

We examined the effect of PAR1 inhibition by P1pal-7 on microvessel density in i.p. ovarian tumors. OVCAR-4 tumors excised from peritoneal organs 6 weeks post-inoculation revealed extensive replacement of normal tissue and had a pronounced serous cyst glandular morphology typical of ovarian adenocarcinoma. We found that P1pal-7 monotherapy caused a highly significant 84% to 96% ($P < 0.005$) reduction in blood vessel density in both the center and the edge of the OVCAR-4 tumors compared with vehicle-treated mice after a treatment period of 6 weeks (Fig. 5A). Likewise, P1pal-7 in combination with docetaxel caused a significant 73% to 92% reduction in blood vessel density in both the center and the edge of the OVCAR-4 tumors compared with docetaxel alone (Fig. 5B). MMP-1 inhibition with FN-439 was found to have similar effects as P1pal-7 on blocking tumor vascularity in the ovarian tumors (Fig. 5B).

Monotherapy with the PAR1 pepducin, P1pal-7, also caused a striking decrease (90%) in mean blood vessel density in i.p. SKOV-3 tumors compared with vehicle-treated mice (Fig. 5C). Addition of P1pal-7 to docetaxel caused a further significant decrease in blood vessel density compared with docetaxel alone. Thus, blockade of PAR1 signaling may provide a benefit in inhibiting angiogenesis either when used alone or in combination with docetaxel in mouse models of peritoneal carcinomatosis.

None of the nude mice that received P1pal-7 every other day for 6 weeks in the presence or absence of docetaxel exhibited any obvious toxicity. To assess whether P1pal-7 was immunogenic or could affect the host immune response, we injected P1pal-7 (10 mg/kg i.p. 6 days/wk) for 6 weeks into DBA/1J mice, which are susceptible to developing autoantibodies and exhibit heightened inflammatory responses. Sera collected at the 6-week time point were not immunoreactive to P1pal-7 by dot-blot compared with vehicle-treated mice (Supplementary Fig. S4A). Moreover, serum KC (Gro-α) levels, a marker of systemic inflammation in mice (26), showed no differences between the P1pal-7 and control groups (Supplementary Fig. S4B). Pepducin-treated mice had normal joint mobility and no evidence of arthritis or swelling over the 6-week period (Supplementary Fig. S4C).

Combination i.p. Therapy of Docetaxel Plus a PAR1-Based Pepducin Inhibits Invasion and Metastasis of Ovarian Cancer in Nude Mice

Patients whose cancer has spread throughout the peritoneal cavity have a survival rate of only 28%; thus, inhibition of peritoneal dissemination and metastatic progression is critical for the successful treatment of ovarian cancer. Docetaxel, or the related paclitaxel administered i.p. and used in combination with other therapies,

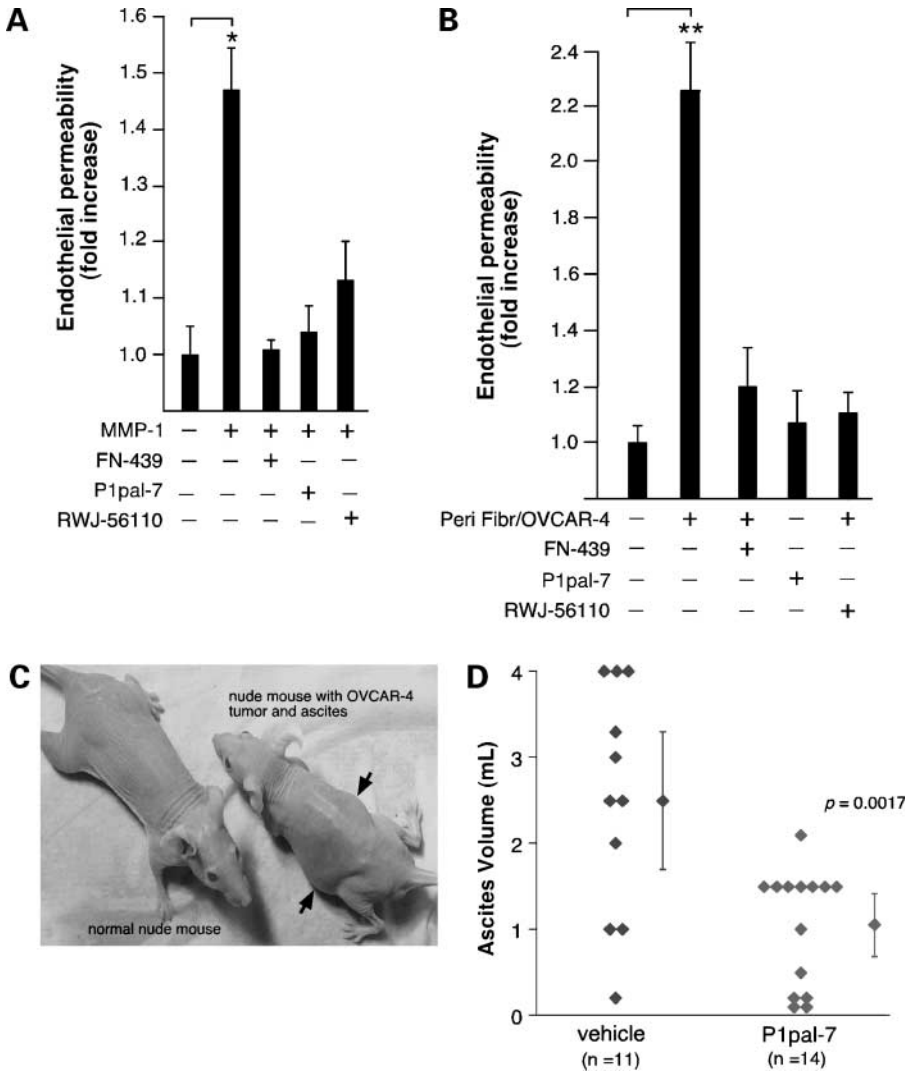

Figure 4. Effects of inhibiting MMP1-PAR1 on endothelial barrier function and ascites production in nude mice with peritoneal ovarian cancer. **A** and **B,** immortalized human umbilical vein endothelial cells (EA.hy926) were grown to confluence on 3 μm polycarbonate Transwell membranes. Endothelium was then stimulated for 2 h with either (**A**) 0.5 nmol/L MMP-1 or (**B**) peritoneal fibroblast conditioned medium harvested after overnight incubation with OVCAR-4 cells in the presence or absence of the MMP-1 antagonist FN-439 (5 μmol/L), the PAR1 antagonist RWJ-56110 (5 μmol/L), or P1pal-7 (3 μmol/L). Evans blue (30 mg/mL in DMEM) was then added to the upper well of the dual chamber system and leakage (15 min) into the bottom well relative to unstimulated control (vascular permeability) was measured by A_{650}. *, $P < 0.05$; **, $P < 0.001$ (n = 3-5 in duplicate). **C,** female NCR *nu/nu* mice were injected i.p. with either RPMI (*left*) or 1.5 million OVCAR-4 cells (*right*) in RPMI. After 40 d, mice injected with cancer cells showed abdominal tumor masses and pronounced ascitic fluid (*arrows*). **D,** female NCR *nu/nu* mice were injected with 1.5 million OVCAR-4 cells and treated with either i.p. vehicle alone (20% DMSO alternate day) or the PAR1 pepducin antagonist P1pal-7 (10 mg/kg alternate day) for 40 d, ascites fluid was collected, and volume was determined.

is emerging as the standard-of-care chemotherapeutic agent for the treatment of advanced and recurrent ovarian cancer (48). Despite the significant inhibitory effects on ascites and angiogenesis, targeting PAR1 alone with P1pal-7 had little effect on the metastatic spread of the OVCAR-4 cells through the peritoneal cavity of the mice (data not shown). It was possible that the residual blood vessels and ascites fluid observed in the mice treated with P1pal-7 alone was sufficient to provide the necessary factors and environment for metastatic progression.

Therefore, we assessed whether inhibition of PAR1 versus MMP-1 in combination with docetaxel was able to slow progression of advanced ovarian cancer in mice. To quantify these effects, we developed a histologic staging system that used the diaphragm as a marker of the progressive invasion and metastasis from the peritoneal cavity/omentum to the thoracic organs (Fig. 6A). Four i.p. treatment groups were evaluated. In the first group, mice received vehicle alone every other day for the 40-day time period. A second group received docetaxel (10 mg/kg) i.p. once weekly starting on day 20 until the end of the 40-day period. The third treatment group received the identical docetaxel regimen plus P1pal-7 (3.2 mg/kg i.p. every other day for 40 days starting 24 h after tumor inoculation to allow implantation). The fourth treatment group received the identical docetaxel regimen plus FN-439 (5 mg/kg i.p. every other day starting 24 h after tumor inoculation). At the 40-day time point, all of the vehicle-treated mice had stage 4 disease with complete penetration through the diaphragm and metastasis to the lungs and mediastinum, confirming that the OVCAR-4 cells were extremely aggressive and metastatic *in vivo*. By comparison, mice treated with docetaxel alone had a marked decrease in metastatic progression, but the cancer had largely spread to the peritoneal surface of the diaphragm (stage Ib; Fig. 6A). Addition of the P1pal-7 pepducin to the docetaxel regimen caused a significant further decrease in invasion ($P = 0.01$) relative to docetaxel alone and slowed invasion into the diaphragm or metastases to the thoracic cavity (Fig. 6B). Likewise, addition of FN-439 to docetaxel conferred

significant ($P = 0.003$) protection against invasion into the diaphragm with no evidence of thoracic metastases.

Targeting the Metalloprotease-PAR1 Axis in Ovarian Cancer

The interaction of ovarian carcinoma cells with peritoneal stromal components, such as fibroblasts and endothelial cells, provides a rich host environment that facilitates tumor growth, invasion, and angiogenesis. MMPs in particular are well adapted to serve as signaling conduits in the tumor-stromal microenvironment given their key roles in the complex processes of tissue invasion, blood vessel homeostasis, and metastasis. MMP-1, MMP-9, and MMP-14 have all been implicated in the progression of ovarian cancer. Our finding that these three stromal and tumor-derived metalloproteases act together in a metalloprotease cascade to activate PAR1 serves to reinforce the notion that carcinoma cells must closely coordinate their malignancy-associated activities with the surrounding stromal cells. The use of membrane-tethered MMP-14, which localizes to the cellular protrusions or invadopodia, might further augment the concentration gradients of the secreted MMP-1 and MMP-9 near the PAR1 receptor and also create an appropriate invasive microenvironment for outward tumor expansion and angiogenesis (49). In addition to MMP-1, PAR1 has several potential protease agonists including thrombin, activated protein C, and plasmin. Thus, downstream blockade of PAR1 with a pepducin might be more advantageous as opposed to direct MMP-1 inhibition, which does not affect other putative PAR1 (serine protease) agonists.

MMP inhibitors are an attractive class of drug candidates for blocking tumor progression, but their approval as cancer therapeutics has been hampered due to toxicity in humans (50). Likewise, i.v. administered chemotherapy

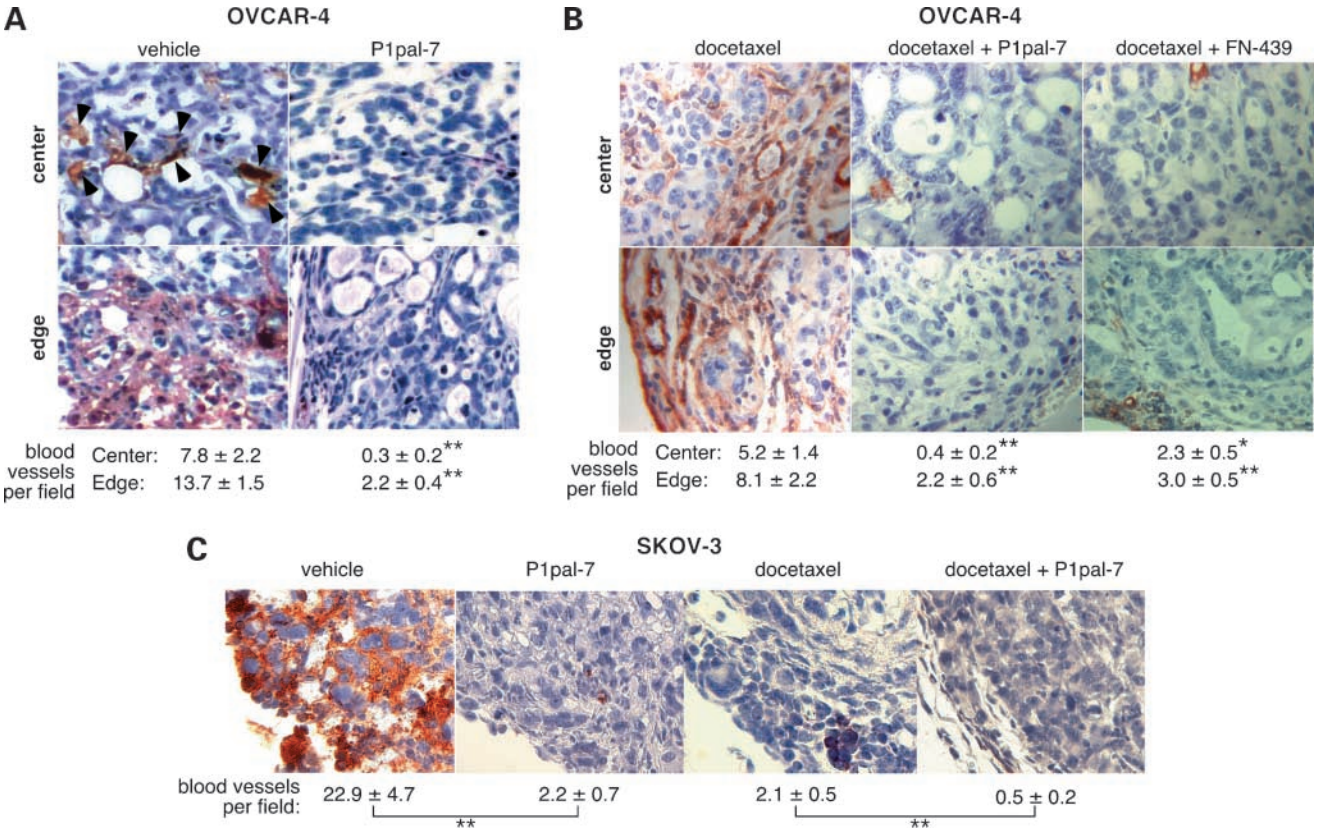

Figure 5. Effects of inhibiting MMP1-PAR1 on angiogenesis in mouse models of peritoneal ovarian cancer. **A** and **B,** PAR1 pepducin, P1pal-7, used either as monotherapy or in combination with docetaxel, inhibits angiogenesis of peritoneal OVCAR-4 cancer in mice. Female NCR *nu/nu* mice were injected i.p. with 1.5 million OVCAR-4 cells and divided into treatment groups of vehicle (10% DMSO alternate day, starting on day 2), P1pal-7 (3.2 mg/kg i.p. alternate day, starting on day 2), docetaxel alone (10 mg/kg) once per week starting at day 20, docetaxel (10 mg/kg) once per week starting at day 20 plus P1pal-7 (3.2 mg/kg i.p. alternate day, starting on day 2), and docetaxel (10 mg/kg) once per week starting at day 20 plus FN-439 (5 mg/kg alternate day, starting on day 2; $n = 8$-10). Intense staining of Weibel-Palade bodies within individual endothelial cells using a rabbit polyclonal anti-von Willebrand factor was scored as a blood vessel in a blinded manner from paraffin-embedded tissue sections from mice with peritoneal OVCAR-4 cancer. Representative sections and blood vessels (*arrowheads*) from tumor centers or tumor edge are shown. Vascular density was determined by counting five to nine fields (magnification, ×160) from at least five tumors in each group. **C,** P1pal-7 inhibits angiogenesis of peritoneal SKOV-3 cancer in mice. Female NCR *nu/nu* mice were injected with 1.5 million SKOV-3 cells and divided into the same four treatment regimens as above ($n = 5$). After 40 d of treatment, the mice were sacrificed, peritoneal tissues were collected for histopathology, and vessel density was assessed as in **A**. *Bottom,* mean blood vessel density per field. *, $P < 0.05$; **, $P < 0.005$.

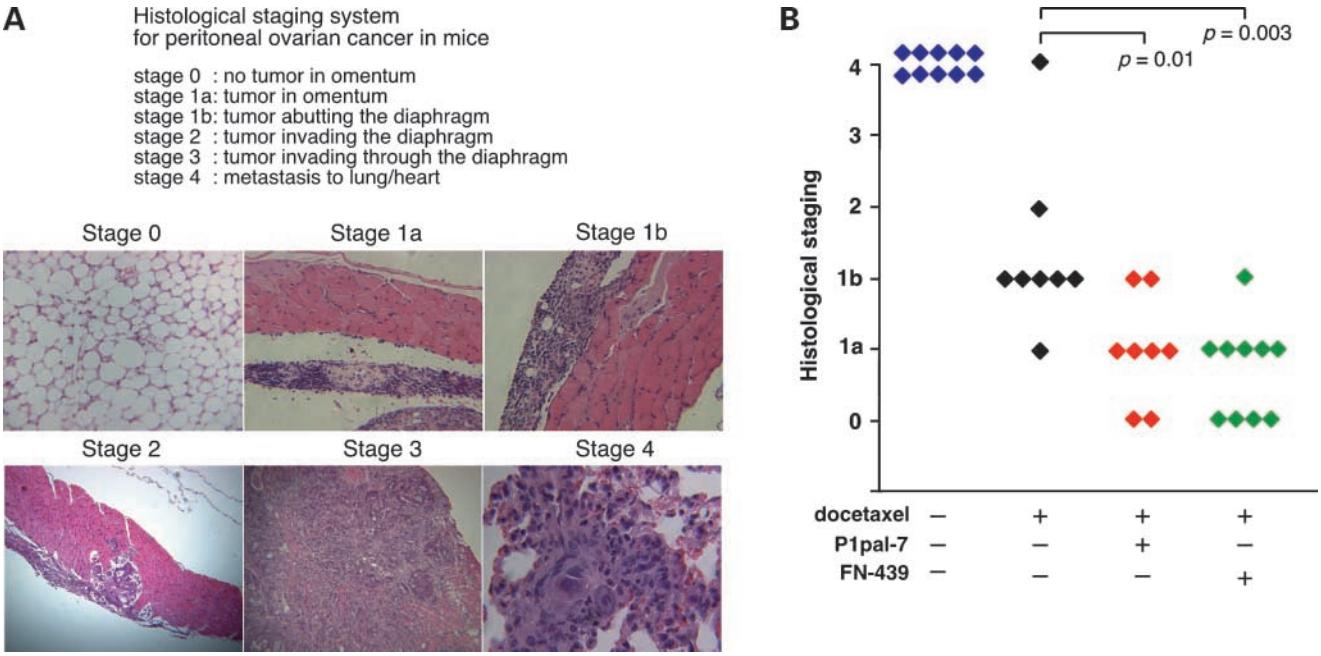

Figure 6. Effect of a PAR1 pepducin in combination with docetaxel on invasion and metastasis in an *in vivo* peritoneal ovarian cancer model. **A,** histologic staging system for peritoneal ovarian cancer in nude mice. **B,** PAR1 pepducin, P1pal-7, or FN-439 MMP-1 inhibitor, used in combination with docetaxel inhibits invasion and metastasis of peritoneal ovarian cancer in mice. Six-week treatment with vehicle, docetaxel alone, or docetaxel plus P1pal-7 or FN-439 was conducted as in Fig. 5A. Mice were euthanized and diaphragm, peritoneal, and thoracic organs were harvested, soaked in 10% formalin, and then sectioned and stained with H&E for histopathologic analyses. Staging was conducted by two independent pathologists who were blinded to the various treatment groups.

often causes severe side effects arising from bone marrow and gastrointestinal toxicity. One strategy to limit systemic side effects and improve tumor targeting in ovarian cancer patients is to deliver the anticancer agent directly to the peritoneal cavity. A recent clinical trial involving 415 patients with stage III ovarian carcinoma randomized patients to standard i.v. versus high-dose i.p. chemotherapy (48). High-dose i.p. cisplatin and paclitaxel significantly increased the overall median survival from 50 to 66 months compared with the i.v. treatment group. Therefore, it anticipated that future treatment regimens for ovarian cancer would further use i.p. therapy. The present study showed that 6-week i.p. administration of a PAR1 pepducin reduced ascites production and angiogenesis and when given in combination with docetaxel inhibited metastatic progression of peritoneal ovarian cancer. An i.p. treatment regimen that targets PAR1 may provide an orthogonal approach by inhibiting both tumor invasion and angiogenesis downstream of MMPs in the peritoneal microenvironment.

Disclosure of Potential Conflicts of Interest

Tufts Medical Center has out-licensed the pepducins used in this paper. No other potential conflicts of interest were disclosed.

Acknowledgments

We thank David Simon for conducting statistical analyses, Yoko Yoda for conducting PCR and fluorescence-activated cell sorting, John Yang, Katie Wakely, and Lawrence Brinkerhoff for providing patient samples, Nga Nguyen for conducting PCR, Claudia Derian and Patricia Andrade-Gordon (Johnson & Johnson Pharmaceuticals) for providing RWJ-56110, and Namita Jain for histopathology analysis.

References

1. Ozols RF, Bookman MA, Connolly DC, et al. Focus on epithelial ovarian cancer. Cancer Cell 2004;5:19 – 24.

2. Sawiris GP, Sherman-Baust CA, Becker KG, Cheadle C, Teichberg D, Morin PJ. Development of a highly specialized cDNA array for the study and diagnosis of epithelial ovarian cancer. Cancer Res 2002;62:2923 – 8.

3. Conrads TP, Fusaro VA, Ross S, et al. High-resolution serum proteomic features for ovarian cancer detection. Endocr Relat Cancer 2004; 11:163 – 78.

4. Egeblad M, Werb Z. New functions for the matrix metalloproteinases in cancer progression. Nat Rev Cancer 2002;2:161 – 74.

5. Pei D. Matrix metalloproteinases target protease-activated receptors on the tumor cell surface. Cancer Cell 2005;7:207 – 8.

6. Naylor MS, Stamp GW, Davies BD, Balkwill FR. Expression and activity of MMPS and their regulators in ovarian cancer. Int J Cancer 1994;58: 50 – 6.

7. Fishman D, Bafetti LM, Banionis S, Kearns AS, Chilukuri K, Stack MS. Production of extracellular matrix-degrading proteinases by primary cultures of human epithelial ovarian carcinoma cells. Cancer 1997;80: 1457 – 1463.

8. Huang LW, Garrett AP, Bell DA, Welch WR, Berkowitz RS, Mok SC. Differential expression of matrix metalloproteinase-9 and tissue inhibitor of metalloproteinase-1 protein and mRNA in epithelial ovarian tumors. Gynecol Oncol 2000;77:369 – 376.

9. Graves LE, Ariztia EV, Navari JR, Matzel HJ, Stack MS, Fishman DA. Proinvasive properties of ovarian cancer ascites-derived membrane vesicles. Cancer Res 2004;64:7045 – 9.

10. Lengyel E, Schmalfeldta B, Konika E, et al. Expression of latent matrix metalloproteinase 9 (MMP-9) predicts survival in advanced ovarian cancer. Gynecol Oncol 2001;82:291 – 8.

11. Huang S, Arsdall MV, Tedjarati S, et al. Contributions of stromal metalloproteinase-9 to angiogenesis and growth of human ovarian carcinoma in mice. J Natl Cancer Inst 2002;94:1134 – 42.

12. Murray GI, Duncan ME, O'Neil P, Melvin WT, Fothergill JE. Matrix metalloproteinase-1 is associated with poor prognosis in colorectal cancer. Nat Med 1996;2:461 – 2.

13. Murray GI, Duncan ME, O'Neil P, McKay JA, Melvin WT, Fothergill JE. Matrix metalloproteinase-1 is associated with poor prognosis in oesophageal cancer. J Pathol 1998;185:256 – 61.

14. van't Veer LJ, Dai H, Vijver MJvd, et al. Gene expression profiling predicts clinical outcome of breast cancer. Nature 2002;415:530 – 6.

15. Poola I, DeWitty RL, Marshalleck JJ, Bhatnagar R, Abraham J, Lefall LD. Identification of MMP-1 as a putative breast cancer predictive marker by global gene expression analysis. Nat Med 2005;11:481 – 3.

16. Rutter JL, Mitchell TI, Buttice G, et al. A single nucleotide polymorphism in the matrix metalloproteinase-1 promoter creates an Ets binding site and augments transcription. Cancer Res 1998;58:5321 – 5.

17. Six L, Grimm C, Leodolter S, et al. A polymorphism in the matrix metalloproteinase-1 gene promoter is associated with the prognosis of patients with ovarian cancer. Gynecol Oncol 2006;100:506 – 10.

18. Boire A, Covic L, Agarwal A, Jacques S, Sharifi S, Kuliopulos A. PAR1 is a matrix metalloprotease-1 receptor that promotes invasion and tumorigenesis of breast cancer cells. Cell 2005;120:303 – 13.

19. Arora P, Ricks TK, Trejo J. Protease-activated receptor signalling, endocytic sorting and dysregulation in cancer. J Cell Sci 2007;120:921 – 8.

20. Even-Ram S, Uziely B, Cohen P, et al. Thrombin receptor overexpression in malignant and physiological invasion processes. Nat Med 1998;4:909 – 14.

21. Grisaru-Granovsky S, Salah Z, Maoz M, Pruss D, Beller U, Bar-Shavit R. Differential expression of protease activated receptor 1 (Par1) and pY397FAK in benign and malignant human ovarian tissue samples. Int J Cancer 2005;113:372 – 8.

22. Covic L, Gresser AL, Talavera J, Swift S, Kuliopulos A. Activation and inhibition of G protein-coupled receptors by cell-penetrating membrane-tethered peptides. Proc Natl Acad Sci U S A 2002a;99:643 – 8.

23. Sanceau J, Truchet S, Bauvois B. Matrix metalloproteinase-9 silencing by RNA interference triggers the migratory-adhesive switch in Ewing's sarcoma cells. J Biol Chem 2003;278:36537 – 46.

24. Ueda J, Kajita M, Suenga N, Fujii K, Seiki M. Sequence-specific silencing of MT1-MMP expression suppresses tumor cell migration and invasion: importance of MT1-MMP as a therapeutic target for invasive tumors. Oncogene 2003;22:8716 – 22.

25. Kuliopulos A, Walsh CT. Production, purification, and cleavage of tandem repeats of recombinant peptides. J Am Chem Soc 1994;116: 4599 – 607.

26. Kaneider NC, Agarwal A, Leger AJ, Kuliopulos A. Reversing systemic inflammatory response syndrome with chemokine receptor pepducins. Nat Med 2005;11:661 – 5.

27. Kamath L, Meydani A, Foss F, Kuliopulos A. Signaling from protease-activated receptor-1 inhibits migration and invasion of breast cancer cells. Cancer Res 2001;61:5933 – 40.

28. Kuliopulos A, Covic L, Seeley SK, Sheridan PJ, Helin J, Costello CE. Plasmin desensitization of the PAR1 thrombin receptor: kinetics, sites of truncation, and implications for thrombolytic therapy. Biochemistry 1999; 38:4572 – 85.

29. Albini A, Benelli R. The chemoinvasion assay: a method to assess tumor and endothelial cell invasion and its modulation. Nat Protocols 2007;2:504 – 11.

30. Covic L, Misra M, Badar J, Singh C, Kuliopulos A. Pepducin-based intervention of thrombin receptor signaling and systemic platelet activation. Nat Med 2002b;8:1161 – 5.

31. Leger A, Jacques SL, Badar J, et al. Blocking the protease-activated receptor 1-4 heterodimer in platelet-mediated thrombosis. Circulation 2006;113:1244 – 54.

32. Covic L, Tchernychev B, Jacques S, Kuliopulos A. In: Pharmacology and in vivo efficacy of pepducins in hemostasis and arterial thrombosis. Langel U, editor. New York: Taylor & Francis; 2006. p. 245 – 57.

33. Andrade-Gordon P, Maryanoff BE, Derian CK, et al. Design, synthesis, and biological characterization of a peptide-mimetic antagonist for a tethered-ligand receptor. Proc Natl Acad Sci U S A 1999;96:12257 – 62.

34. Nguyen N, Kuliopulos A, Graham RA, Covic L. Tumor-derived Cyr61(CCN1) promotes stromal matrix metalloprotease-1 production and protease-activated receptor 1-dependent migration of breast cancer cells. Cancer Res 2006;66:2658 – 65.

35. Davidson B, Goldberg I, Gotlieb WH, Ben-Baruch G, Nesland JM, Reich R. The prognostic value of metalloproteinase and angiogenic factors in ovarian cancer. Mol Cell Endocrinol 2002;187:39 – 45.

36. Drew AF, Blick TJ, Lafleur MA, et al. Correlation of tumor- and stromal-derived MT1-MMP expression with progression of human ovarian tumors in SCID mice. Gynecol Onc 2004;95:437 – 48.

37. Cao J, Rehemtulla A, Bahou W, Zucker S. Membrane type matrix metalloproteinase 1 activates pro-gelatinase A without furin cleavage of the N-terminal domain. J Biol Chem 1996;271:30174 – 80.

38. Sternlicht MD, Werb Z. How matrix metalloproteinases regulate cell behavior. Annu Rev Cell Dev Biol 2001;17:463 – 516.

39. Wang P, Nie J, Pei D. The hemopexin domain of membrane-type matrix metalloproteinase-1 (MT1-MMP) Is not required for its activation of proMMP2 on cell surface but is essential for MT1-MMP-mediated invasion in three-dimensional type I collagen. J Biol Chem 2004; 279:51148 – 55.

40. Murphy G, Knauper V, Cowell S, et al. Evaluation of some newer matrix metalloproteinases. Ann NY Acad Sci 1999;878:25 – 39.

41. Nagy JA, Masse EM, Herzberg KT, et al. Pathogenesis of ascites tumor growth: vascular permeability factor, vascular hyperpermeability, and ascites fluid accumulation. Cancer Res 1995;55:360 – 8.

42. Mesiano S, Ferrara N, Jaffe RB. Role of vascular endothelial growth factor in ovarian cancer. Am J Pathol 1998;153:1249 – 56.

43. Garcia JG, Davis HW, Patterson CE. Regulation of endothelial cell gap formation and barrier dysfunction: role of myosin light chain phosphorylation. J Cell Physiol 1995;163:510 – 22.

44. Klarenbach SW, Chipiuk A, Nelson RC, Hollenberg MD, Murray AG. Differential actions of PAR2 and PAR1 in stimulating human endothelial cell exocytosis and permeability: the role of Rho-GTPases. Circ Res 2003; 92:272 – 8.

45. Kaneider NC, Leger AJ, Agarwal A, et al. Role reversal for the receptor PAR1 in sepsis-induced vascular damage. Nat Immunol 2007;8: 1303 – 12.

46. Goerge T, Barg A, Schnaeker E-M, et al. Tumor-derived matrix metalloprotease-1 targets endothelial proteinase-activated receptor 1 promoting endothelial cell activation. Cancer Res 2006;66:7766 – 74.

47. Suganuma T, Ino K, Shibata K, et al. Functional expression of the angiotensin II type 1 receptor in human ovarian carcinoma cells and its blockade therapy resulting in suppression of tumor invasion, angiogenesis, and peritoneal dissemination. Clin Cancer Res 2005;11:2686 – 94.

48. Armstrong DK, Bundy B, Wenzel L, et al. Intraperitoneal cisplatin and paclitaxel in ovarian cancer. N Engl J Med 2006;354:34 – 43.

49. Hotary K, Li X-Y, Allen E, Stevens SL, Weiss SJ. A cancer cell metalloprotease triad regulates the basement membrane transmigration program. Genes Dev 2006;20:2673 – 86.

50. Coussens LM, Fingleton B, Matrisian LM. Matrix metalloproteinase inhibitors and cancer: trials and tribulations. Science 2002;295: 2387 – 92.

Molecular Cancer Therapeutics

Targeting a metalloprotease-PAR1 signaling system with cell-penetrating pepducins inhibits angiogenesis, ascites, and progression of ovarian cancer

Anika Agarwal, Lidija Covic, Leila M. Sevigny, et al.

Mol Cancer Ther 2008;7:2746-2757.